A modified explanation of cold nuclear matter effects on J/ψ production in p+A collisions*

LIU Zhi-Feng(刘植风)[1)]
Institute of Geophysics, Shijiazhuang Economic University, Shijiazhuang, China

Abstract: A modified explanation of the cold nuclear matter (CNM) effects on J/ψ production in p+A collisions is presented in this paper. The advantage of the modified explanation is that all the CNM effects implemented in this model have clear physical origins and are mostly centered on the idea of multiple parton scattering. With the CNM effects presented in this paper, we calculated the nuclear modification factor $R_{\rm pA}$ in J/ψ production under different collision energies. The results are compared with the corresponding experiment data and the factors calculated with classic nuclear effects. The factors calculated with CNM effects presented in this paper can accurately reproduce almost all existing J/ψ measurements in p-A collisions, which is much better than results obtained with the factors calculated with classic nuclear effects. The new model is therefore a more suitable approach to explain CNM effects in the hardproduction of quarkonium.

Key words: quantum chromodynamics, cold nuclear matter effects, quark energy loss effect, dynamical shadowing effect, gluon saturation

PACS: 13.85.Ni **DOI:** 10.1088/1674-1137/39/8/084104

1 Introduction

Quarkonium production in heavy ion collisions, such as the production of J/ψ, is a vital testing ground for novel nontrivial QCD dynamics (p+A). By studying the medium-induced modification of quarkonium production in nucleus collisions (p+A) relative to naive proton-proton collisions (p+p), one can get information on the novel nontrivial QCD dynamics, especially with the process in d+Au collisions at RHIC and the forthcoming p+Pb collisions at LHC. The manifestations of such nontrivial QCD dynamics in p+A reactions are usually called cold nuclear matter (CNM) effects - those effects cause an obvious suppression of cross section, but not because of the formation of quark-gluon plasma.

There have been several approaches to study CNM effects in the past decade. One approach is based on perturbative QCD factorization and attributes all these effects to universal nuclear parton distribution functions (nPDFs). With this approach Eskola and Hirai et al fixed the parametrizations of nPDFs through a global fitting procedure [1, 2], where those nPDFs become the only ingredients that were different from the case of p+p collisions. This approach can describe part of the RHIC d+Au data reasonably well. Another approach is the so-called Color Glass Condensate (CGC) approach [3]. Because it focuses on non-linear corrections to QCD evolution equations in very dense gluonic systems and is only applicable in the very small-x region, the CGC approach is not as popular as the perturbative QCD method. There are also calculations and predictions for the nuclear modification factor in Monte Carlo models such as HIJING.

In this paper we followed a new approach derived from multiple parton scattering theory. This approach is based on perturbative QCD factorization. At the same time, CNM effects are implemented separately within the formalism by modification of the corresponding variables. The advantage of this approach is that all CNM effects have a clear physical origin and are mostly centered on the idea of multiple parton scattering [4]. This approach was first derived in Ref. [5]. In Ref. [5] the cross section data of prompt photons in p+A collisions at RHIC was reproduced perfectly with this approach (see Fig. 1, Fig. 2 in Ref. [5]). In their calculation the isospin effect, Cronin effect, CNM energy loss, and dynamical shadowing were included.

In this manuscript we will improve their model and calculate the production cross section ratio of J/ψ in p+A collisions. As we know, according to multiple parton scattering theory, under some approximate conditions, at sufficiently large quarkonium energy E in the

Received 20 November 2014
∗ Supported by National Nature Science Foundation of China (10575028)
1) E-mail: liuzhifeng_cc@163.com

target rest frame, quarkonium hadroproduction looks like small angle scattering of a color charge [6]. Based on this theory, we used a new CNM energy loss model derived from the medium-induced gluon radiation spectrum (similar to the Bethe-Heitler spectrum) to calculate the fractional energy loss ε [6], which is different from the effective reduced fractional energy loss $\varepsilon_{\rm eff}$ used in [5]. Because our calculation of ε has included the effects of the transverse momentum nuclear broadening, we do not discuss the Cronin effect separately in the following sections. In fact, considering the high collision energy in p+A collisions, which means that partons undergoing hard collisions are in a very small-x region (for example, about 10^{-4} at LHC), the gluon saturation effect was included in our calculation within the so-called classic gluon saturation regime [7]. In the following, Section 2 introduces the CNM effects. In Section 3 the results and conclusion are presented.

2 Cold nuclear matter effects

In general, the CNM effects in p+A collisions can be quantified with a nuclear modification factor $R_{\rm pA}$, which is usually defined as:

$$R_{\rm pA}=\frac{1}{A}\frac{{\rm d}\sigma_{\rm pA}}{{\rm d}y{\rm d}^2p_{\rm T}}/\frac{{\rm d}\sigma_{\rm pp}}{{\rm d}y{\rm d}^2p_{\rm T}}. \tag{1}$$

Here A is the nucleon number of the target nucleus. The deviation of $R_{\rm pA}$ from unity reveals the presence of CNM effects in p+A collisions.

A variety of CNM effects can affect particle production. In this paper we mainly discuss those effects that have been theoretically evaluated as arising from the elastic, inelastic and coherent scattering of partons in large nuclei [4].

Within the perturbative QCD factorization approach there have been different ways to calculate heavy quark production. In this paper, the heavy quark production in p+p collisions was calculated with the Color Octet Model (COM). According to this model, the differential production cross section for a charmonium state can be written as:

$$\begin{aligned}\frac{{\rm d}\sigma_{{\rm J}/\psi}}{{\rm d}y} &= \frac{{\rm d}\sigma({\rm J}/\psi)_{\rm dir}}{{\rm d}y}\\ &\quad+\sum_{J=0,1,2}Br(\chi_{\rm cJ}\rightarrow{\rm J}/\psi X)\frac{{\rm d}\sigma(\chi_{\rm cJ})}{{\rm d}y}\\ &\quad+Br(\psi'\rightarrow{\rm J}/\psi X)\frac{{\rm d}\sigma(\psi')}{{\rm d}y},\end{aligned} \tag{2}$$

where Br is the branching ratio [8]. The rapidity distribution of particle C in the final state is as follows [9]:

$$\begin{aligned}&f_{\rm i}^{\rm N}(x_1,Q^2)f_{\rm j}^{\rm N}(x_2,Q^2)\frac{{\rm d}\sigma_{\rm i,j}^{\rm C}}{{\rm d}y}\\ &=\sum_{\rm i,j}\sum_{\rm n}\int_0^1{\rm d}x_1{\rm d}x_2\delta\left(y-\frac{1}{2}\ln\left(\frac{x_1}{x_2}\right)\right)\\ &\quad\times f_{\rm q}^{\rm N}(x_1,Q^2)f_{\bar{\rm q}}^{\rm N}(x_2,Q^2)C^{\rm ij}_{{\rm Q\bar{Q}[n]}}\langle\vartheta_{\rm n}^{\rm C}\rangle.\end{aligned} \tag{3}$$

The sum over i and j includes all the partons (quark, antiquark and gluon).

In Fig. 1 the distribution of ${\rm d}\sigma/{\rm d}y$ vs. rapidity (y) for J/ψ production in p+p collisions at RHIC is presented. The results calculated with GRV LO98 (solid line) and HKN07 (dashed line) can all reproduce most of the data within the error range. In the following study of the nuclear modification factor we therefore take the results calculated with COM (HKN07) in p+p collisions as a baseline.

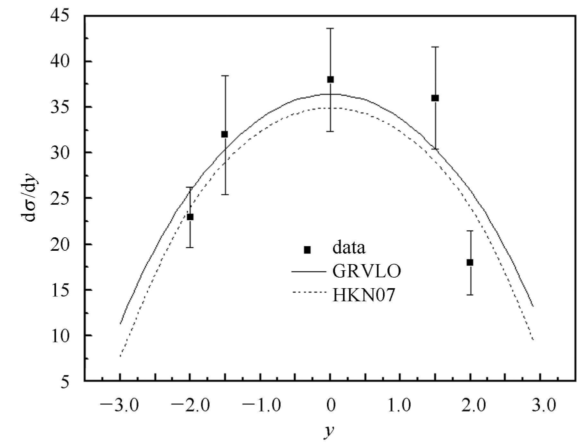

Fig. 1. Rapidity distribution of ${\rm d}\sigma/{\rm d}y$ at PHENIX [10].

2.1 Cold nuclear matter energy loss

The CNM energy loss effect can be easily implemented as a momentum fraction shift in the PDFs of the incoming proton. According to multiple parton scattering theory, as the parton from the proton undergoes multiple scattering in the nucleus before the hard collisions, it can lose energy due to medium-induced gluon bremsstrahlung, which corrects the momentum fraction in the PDFs of the incoming proton with a shift ε [5]:

$$\begin{aligned}&f_{\rm q/p}(x_{\rm a},Q^2)\rightarrow f_{\rm q/p}\left(\frac{x_{\rm a}}{1-\varepsilon},Q^2\right),\\ &f_{\rm g/p}(x_{\rm a},Q^2)\rightarrow f_{\rm g/p}\left(\frac{x_{\rm a}}{1-\varepsilon},Q^2\right).\end{aligned} \tag{4}$$

Here $\varepsilon=\langle\sum_i\omega_i/E\rangle$ is the average fractional energy loss induced by multiple gluon emission. The sum runs over all medium-induced gluons. Ideally, Eq. (4) should include a convolution over the probability distribution of CNM energy loss $P_{\rm q,g}(\varepsilon)$ [11]. The probability distribution $P_{\rm q,g}(\varepsilon)$ is calculated for quarks and gluons separately in the Poisson approximation [12]. This calculation of initial-state CNM energy loss has been shown to give a good description of the nuclear modification of Drell-Yan production in fixed target experiments [13].

Instead of using an effective reduced fractional energy loss $\varepsilon_{\rm eff}$ as in Ref. [5], the calculation of ε in this paper follows the method in Ref. [6]. In their paper they assumed that the heavy-quark $\mathrm{Q\bar{Q}}$ pair is produced in a compact color octet state within the hard process time-scale $t_{\rm h}$, and remains a color octet for a time much longer than $t_{\rm h}$. In quarkonium production models where color neutralization is a soft non-perturbative process, this assumption holds at any $x_{\rm F}$. With this assumption, at sufficiently large quarkonium energy E in the target rest frame, quarkonium hadroproduction looks like small angle scattering of a color charge [6]. So the medium-induced initial-state radiation spectrum is similar to the Bethe-Heitler spectrum and is written as follows [6]:

$$\omega\frac{\mathrm{d}I}{\mathrm{d}\omega}=\frac{N_{\rm c}\alpha_{\rm s}}{\pi}\left\{\ln\left(1+\frac{\Delta q_{\perp}^2E^2}{M_{\perp}^2\omega^2}\right)-\ln\left(1+\frac{\Lambda^2E^2}{M_{\perp}^2\omega^2}\right)\right\}. \quad (5)$$

Here $\Delta\hat{q}_{\perp}^2$ is the transverse momentum nuclear broadening, which is a variable related to the Cronin effect. $M_{\perp}=\sqrt{M^2+p_{\perp}^2}$ is the transverse mass. M=3 GeV is the mass of a compact $\mathrm{c\bar{c}}$ pair. The average initial-state radiative energy loss can be obtained by integrating the medium-induced bremsstrahlung spectrum [14]:

$$\Delta E\equiv\int_0^E\mathrm{d}\omega\omega\frac{\mathrm{d}I}{\mathrm{d}\omega}\approx N_{\rm c}\alpha_{\rm s}\frac{\sqrt{\hat{q}_A(x)L}}{M_{\perp}}E. \quad (6)$$

The average path length L is given by $L=\frac{3}{2}r_0A^{1/3}$. $\hat{q}_A(x)$ stands for the transport coefficient in nucleus A and is related to the gluon distribution $G(x)$ in the target nucleon as [15]:

$$\hat{q}(x)=\frac{4\pi^2\alpha_{\rm s}(\hat{q}L)N_{\rm c}}{N_{\rm c}^2-1}\rho xG(x,\hat{q}L)\approx\frac{4\pi^2\alpha_{\rm s}N_{\rm c}}{N_c^2-1}\rho xG(x). \quad (7)$$

Here ρ is the target nuclear density. $\alpha_{\rm s}$ is the running parameter. $N_{\rm c}$ is the number of colors.

In the present study we have assumed for simplicity that the octet $\mathrm{Q\bar{Q}}$ pair arises dominantly from the splitting of an incoming gluon. This should be a valid assumption for all p+A data considered in this paper, except at very large values of $x_{\rm F}$ ($x_{\rm F}>0.8$), where quark-induced processes come into play.

The energy loss model used in this paper is based on multiple parton scattering theory and is calculated with an integration of the initial-state medium-induced bremsstrahlung spectrum. It has a clear physical origin that is different from the classic energy loss model [16].

2.2 Dynamical shadowing effect

Power-suppressed coherent final-state scattering of the struck partons leads to suppression of the cross section in the small-x region, which is called the dynamical shadowing effect. This effect represents the interactions between the scattering partons and the nuclear background chromo-magnetic field. So, analogous to the generation of dynamical mass for electrons propagating in a strong electro-magnetic field, the dynamical shadowing effect can be interpreted as a generation of dynamical parton mass in the background gluon field of the nucleus, and contributes to the cross section at the power corrections level with a modification to Bjorken $x_{\rm b}$ of the target nucleus [11]. Such a correction leads to a suppression of the single and double inclusive hadron production cross sections at forward rapidity as long as the coherence criterion is satisfied.

The dynamical parton mass, which is calculated in QCD, is given by $m_{\rm dyn}^2=\zeta^2(A^{1/3}-1)$ [17]. Then the corresponding change in the value of Bjorken $x_{\rm b}$ is

$$x_{\rm b}\rightarrow x_{\rm b}\left(1+\frac{m_{\rm dyn}^2}{Q^2}\right). \quad (8)$$

In the case of the production of J/ψ, the nuclear size enhanced ($A^{1/3}$) power correction can be resumed for a given partonic channel (t-channel) and lead to the following shift in the momentum fraction $x_{\rm b}$ for the parton inside the nucleus [6]:

$$x_{\rm b}\rightarrow x_{\rm b}\left(1+C_{\rm d}\frac{\xi^2(A^{1/3}-1)}{-\hat{t}}\right). \quad (9)$$

Here $x_{\rm b}$ is the parton momentum fraction inside the target nucleus, and $C_{\rm d}=C_{\rm F}(C_{\rm A})$ if the parton $d=q(g)$ in the partonic scattering ab→cd. ξ^2 stands for a characteristic scale of the multiple scattering per nucleon [18]. For $x_{\rm b}<0.1$, due to coherence, $m_{\rm dyn}^2$ has to be incorporated in the underlying kinematics of the hard scattering in Eq. (8); for $x_{\rm b}>0.1$, because the vector meson exchange is localized to one nucleon, the elastic final-state interactions vanish.

Similar shifts in the momentum fraction $x_{\rm b}$ can be obtained easily from Eq. (9) by substituting $\hat{t}\rightarrow\hat{u}$ or $\hat{t}\rightarrow\hat{s}$ respectively in other partonic channels [19].

In short, the dynamical shadowing effect presented in this paper represents the interactions between the scattering outgoing partons and the nuclear background chromo-magnetic field, which leads to a shift in the momentum fraction $x_{\rm b}$ inside the target nucleus. Comparing with the classic shadowing effect defined as the ratio of PDFs in nucleus vs. PDFs in proton [1, 2], the dynamical shadowing effect has a clearer physical origin.

2.3 Gluon saturation effect

Because the parton momentum fraction x probed in collisions at RHIC and LHC is very small, the gluon saturation effect must be included in our calculation. At small values of x, parton wave functions inside the nucleus start to overlap, which changes the effective collision number in the nucleus and leads to an additional J/ψ suppression in high-energy p+A collisions. This phenomenon is named the gluon saturation effect. The suppression here is independent of that caused by the energy loss effect discussed above. In fact, because the saturation effect is expected to scale roughly as the nucleus transverse density, $V/S\sim A^{1/3}$, the J/ψ normalized yield in p+A collisions is likely to be suppressed with respect to that in p+p collisions either at large $x_{\rm F}$ and/or at high energies.

In the present paper, we shall implement the physics of saturation following the work of Fujii, Gelis and Venugopalan [7], where J/ψ suppression has been calculated within the Color Glass Condensate assuming 2→1 kinematics for the J/ψ production process. The nuclear suppression is a scaling function of the saturation scale $Q_{\rm s}$, which can be simply parameterized as:

$$S_{\rm A}^{{\rm J}/\psi}(x_2,L)\approx\left(1+\frac{Q_{\rm s}^2(x_2,L)}{b}\right)^{-\alpha}. \quad (10)$$

Here b=2.65 GeV^2 and α=0.417. The saturation scale $Q_{\rm s}$ is determined through the relationship [20]:

$$Q_{\rm s}^2(x,L)=\hat{q}(x)L. \quad (11)$$

$\hat{q}(x)$ is the transport coefficient and L is the average path length. Both of these have been presented above in Section 2.1.

3 Conclusion

In order to verify the applicability of the new CNM effect model in explaining the production suppression in p+A collisions, the cross section ratios of J/ψ under different collision energies were calculated. The new model is based on multiple parton scattering theory and includes the CNM effects including energy loss effect, isospin effect, dynamical shadowing effect and gluon saturation. The results calculated with the new model were compared with the experiment data collected under different collision energies as well as the results calculated with the classic nuclear effect model. With the classic nuclear effect model, we calculated the energy loss effect with the GM model [16], shadowing effects with EPS09 [1] and the final-state nuclear absorption effect with the Glauber model [21].

In Fig. 2 the rapidity distribution of the nuclear modification factor $R_{\rm Au/p}$ under RHIC collision energy is plotted. As can be seen from Fig. 2, the agreement between the result calculated with the new model (dashed line) and the experiment data [22] is very good over a wide range in y, both in shape and magnitude, while a slight disagreement is observed below $y<-2$, where nuclear absorption is expected to play a role. Compared with the new model, the result calculated with the classic model (solid line) has an obviously bigger error, which indicates that the new model is more suitable to explain the CNM effect in J/ψ production at RHIC. In Fig. 2 we also plot the results calculated with energy loss plus dynamical shadowing (dotted line) and that of energy loss plus the saturation effect (short dash-dotted line). The dotted line is above the short dash-dotted line at forward rapidity, which indicates that, compared with the dynamical shadowing effect, the gluon saturation effect plays a more important role in the production suppression in the corresponding momentum fraction range.

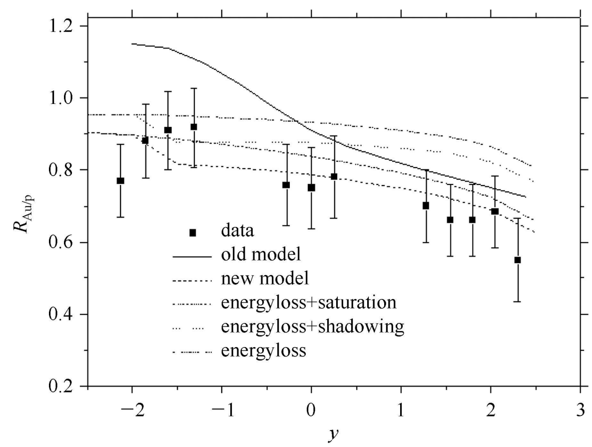

Fig. 2. Rapidity distribution of $R_{\rm Au/p}$ at PHENIX.

In Fig. 3 the $x_{\rm F}$ distribution of nuclear modification factor $R_{\rm W/Be}$ under E866 collision energy is plotted. Here the dashed line represents the result calculated with the new model while the solid line represents that of the classic model. As can be seen from Fig. 3, the agreement between the dashed line and data [23] is excellent both in shape and magnitude over a wide range, while an obvious disagreement is observed above $x_{\rm F}>0.7$, where quark-induced processes start to dominate. In Fig. 3 we also plot the results calculated with energy loss plus dynamical shadowing (dotted line) and that of energy loss plus saturation effect (short dash-dotted line). Both of the lines are similar over the whole $x_{\rm F}$ range, which hints at the equal importance of the two effects in this momentum fraction range. The difference between the dashed line and dotted lines at E866 is smaller than that at RHIC, which may be due to a weaker dynamical shadowing effect under lower collision energy.

In Ref. [6] the effects of CNM energy loss on J/ψ suppression in p+A collisions are studied with the associated soft gluon radiation spectrum. The distribution of nuclear modification factor $R_{A/B}$vs. $x_F(y)$ for E866 (Fig. 1 in Ref. [6]) and RHIC (Fig. 3 in Ref. [6]) are presented respectively. Compared with their results, we find that the fitting to the RHIC data in this paper (Fig. 2) is much better than that in Ref. [6] (Fig. 3), especially across almost the whole $-y$ range, which hints at the importance of the dynamical shadowing effect within the $-y$ range. Apart from that, the results for E866 in both papers are similar. Both Fig. 3 in this paper and Fig. 1 in Ref. [6] can basically reproduce the data in E866 except in the range $x_F > 0.8$.

In Fig. 4 the x_F distribution of nuclear modification factor $R_{w/c}$ under HERA collision energy is plotted. As can be seen from Fig. 4, the line calculated with the new model reproduces the data [24] excellently both in shape and magnitude, much better than that with the classic model - the latter only reproduces the magnitude of the data.

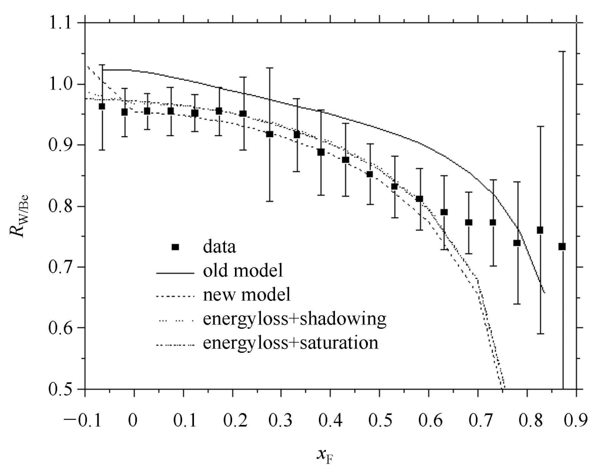

Fig. 3. x_F distribution of $R_{W/Be}$ at E866.

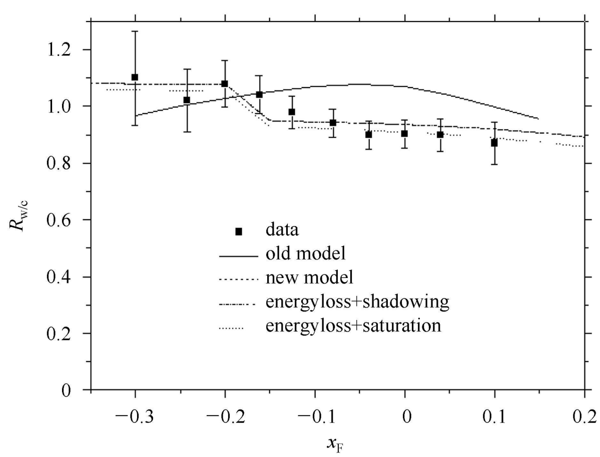

Fig. 4. x_F distribution of $R_{w/c}$ at HERA.

Obviously, compared with the classic model, the new model is able to reproduce the cross section suppression in p+A collisions under different collision energies more accurately, both in magnitude and shape. It should therefore be more suitable to explain the CNM effects in J/ψ production.

Finally, the rapidity dependence of J/ψ suppression in p-Pb collisions at LHC is shown in Fig. 5. Here the dashed line represents the result calculated with the new model while the solid line represents that of the classic model. Both lines are similar in shape and magnitude, except that the dashed line is lower than the solid line. As this is only a prediction, our result needs to be tested with the future experiment data.

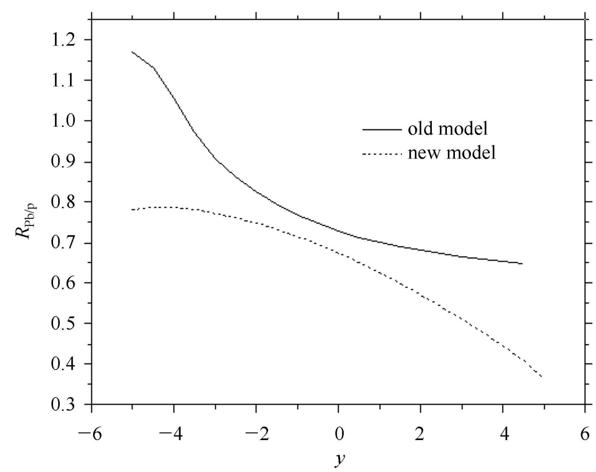

Fig. 5. Rapidity distribution of $R_{Pb/p}$ at LHC.

In summary, the cross section ratio of J/ψ produced in p+A collisions was calculated with a new nuclear effects model in this paper, which includes CNM effects such as the energy loss effect, isospin effect, gluon saturation effect and dynamical shadowing effect. The advantage of this new model is that all CNM effects have clear physical origins and are mostly centered on the idea of multiple parton scattering. It is proved that the results calculated with this new model are able to reproduce accurately almost all existing J/ψ measurements in p+A collisions. In particular, the dependence of J/ψ suppression on x_F/y is well accounted for by this model for various atomic mass A and center-of-mass energies. These results eventually verified the applicability of the new CNM effect model in explaining the CNM effects on J/ψ production. In future, we will investigate CNM effects with this new model on production of other particles in heavy-ion collisions.

We are very grateful to N. Liu and L. H. Song for our fruitful discussions.

References

1 Eskola K J, Paukkunen H, Salgado C A. JHEP, 2009, **0904**: 065
2 Hirai M, Kumano S, Nagai T H. Phys. Rev. C, 2007, **76**: 065207
3 Barnafoldi G G et al. Phys. Rev. C, 2012, **85**: 024903
4 Vitev I et al. Phys. Rev. D, 2006, **74**: 054010
5 KANG Z B, Vitev I, XING H X. Phys. Lett. B, 2012, **718**: 482
6 Arleo F, Peigne S. Phys. Rev. Lett., 2012, **109**: 122301
7 Fujii H, Gelis F, Venugopalan R. Nucl. Phys. A, 2006, **09**: 012
8 Maltoni F et al. Phys. Lett. B, 2006, **638**: 202–208
9 Emel'yanov V, Klein S R, Vogt R. Phys. Rev. C, 2000, **61**: 044904
10 Cooper F, LIU X M, Nayak G C. Phys. Rev. Lett., 2004, **93**: 171801
11 KANG Z B, Vitev I, XING H X. Phys. Rev. D, 2011, **85**: 054024
12 Vitev I. Phys. Lett. B, 2006, **639**: 38
13 Neufeld R B, Vitev I, ZHANG B W. Phys. Lett. B, 2011, **704**: 590
14 Arleo F, Peigne S, Sami T. Phys. Rev. D, 2011, **83**: 114036
15 Baier R et al. Nucl. Phys. B, 1997, **484**: 265
16 Baier R et al. Nucl. Phys. B, 1998, **531**: 403
17 QIU J W, Vitev I. Phys. Rev. Lett., 2004, **93**: 262301
18 Sharma R, Vitev I, ZHANG B W. Phys. Rev. C, 2009, **80**: 054902
19 Vitev I, Goldman T, Johnson M B. Phys. Rev. D, 2006, **74**: 054010
20 Baier R. Nucl. Phys. A, 2003, **715**: 209
21 Shahoyan R. Measurement of Nuclear Effects in the Production of J/ψ Mesons with the HERA–B Detector (Ph. D. Thesis). Portugal: Universidade Tecnica de Lisboa, 2005
22 Adare A et al. Phys. Rev. Lett., 2011, **107**: 142301
23 Leitch M J et al. Phys. Rev. Lett., 2000, **84**: 3256
24 Abt I et al. (HERA-B collaboration). Eur. Phys. J. C, 2009, **60**: 525